JOURNAL OF GUIDANCE, CONTROL, AND DYNAMICS
Vol. 28, No. 4, July–August 2005

Fuel-Optimal Transfers Between Coplanar Circular Orbits Using Variable-Specific-Impulse Engines

Hans Seywald*
Analytical Mechanics Associates, Inc., Hampton, Virginia 23666
Carlos M. Roithmayr† and Patrick A. Troutman‡
NASA Langley Research Center, Hampton, Virginia 23681-2199
and
Sang-Young Park§
Yonsei University, Seoul 120-749, Republic of Korea

Minimum fuel circular-to-circular low-thrust orbital transfers with prescribed transfer time and with the thrust always directed parallel to the velocity vector are developed for a variable-specific-impulse system. The changeable specific impulse serves as the control variable. The power input is assumed to be constant, and the resulting thrust magnitude is inversely proportional to the chosen specific impulse. With these engine specifications, and under the assumption that the thrust magnitude always remains small compared to the gravitational forces, it is shown that the optimal specific impulse profile increases linearly with time. The associated optimal thrust magnitude is proportional to the vehicle mass; that is, the thrust per unit of vehicle mass remains constant. The mass fraction obtained with variable specific impulse is shown to be greater than or equal to that obtained with constant specific impulse; the advantage can be significant for orbital transfers with large changes in the semimajor axis.

I. Introduction

THE Variable Specific Impulse Magnetoplasma Rocket (VASIMR)[1,2,¶] engine under development at the NASA Johnson Space Flight Center is an example of a next-generation electric propulsion system in the variable-specific-impulse class. In contrast to the well-known ion thrusters or Hall thrusters, the VASIMR engine accelerates plasma not along a linear path but along a spiral path, much like in a cyclotron. The longer the plasma is kept magnetically trapped on its spiral path before it is expelled through a magnetic nozzle, the more energy is deposited in the accelerated mass, and the higher is the exhaust velocity. It is expected that this physical setup will enable extremely high specific impulses of up to 30,000 s.

Clearly, the new design also adds the inherent capability to "throttle" the engine. It is anticipated that, by controlling the magnetic nozzle that releases the plasma from its spiral path into a linear exhaust nozzle, the specific impulse can be throttled between 3000 and 30,000 s. Given a constant input power from solar panels or a nuclear reactor, the thrust is inversely proportional to the specific impulse. Obviously, the longer the plasma is kept trapped on its spiral path, the larger is the specific impulse, and the smaller is the mass flow and the thrust.

The low-thrust escape or capture trajectory can have many hundreds of revolutions around the central body because the low thrust is relatively very small compared to the gravitational force of the central body. Hence, it is very difficult and time consuming to find the optimal low-thrust trajectory near the central body by numerical means when the thrust direction is variable and even more difficult when the thrust magnitude is also variable. To overcome the difficulties in numerical studies, it is necessary to develop analytical solutions to obtain insights into the optimal trajectory of a spacecraft with a variable thrust engine. Previous related work is described as follows. In Ref. 3, Battin analytically determines the flight time and the approximate number of revolutions required to escape a planet by using constant tangential thrust acceleration. Stewart and Melton apply perturbation analysis methods in Ref. 4 to a constant low-thrust trajectory and derive approximate analytical solutions. Approximate formulas for minimum-time, constant tangential low-thrust trajectories near an oblate planet are obtained by Sukhanov and Prado in Ref. 5. The problem of minimum-time low-thrust travel is treated by Kiforenko et al. with the averaging method to obtain an analytical approximation in Ref. 6. An analytical solution of a low-thrust transfer orbit yields the evolutions of orbital elements caused by constant thrust, as shown by Xin and Lin in Ref. 7. The analytical solutions obtained in the foregoing references are all associated with constant thrust. For variable thrust magnitude, a first-order analytical solution is developed in terms of the imposed changes on the orbital elements.[8] That analysis is complicated and somewhat impractical because it considers changes in all of the orbital elements. Thus, in this paper we develop simple and reasonably accurate analytical solutions to low-thrust escape and capture trajectories with variable thrust magnitude.

In the absence of any constraints on the time required to perform a given orbital transfer, it is always optimal to operate the engine at its highest possible specific impulse. However, if time constraints are present, it might be necessary to trade some of the specific impulse in return for higher thrust. The main objective of the present paper is to optimize this tradeoff for a particular mission.

Explicitly, the current paper is concerned with finding the optimal specific-impulse profile and the associated thrust profile that minimizes the overall fuel consumption required for a time-constrained, planar, circular-to-circular low-thrust orbital transfer. The optimization is performed in two steps. First, a simplified dynamical system is derived based on the assumption that the thrust is always small in magnitude and that the thrust direction is always the same as, or opposite to the velocity vector direction. For this simplified dynamical system, the overall velocity increment required to perform the

Presented as Paper 2003-0122 at the AAS/AIAA Space Flight Mechanics Meeting, Ponce, PR, 9–13 February 2003; received 24 December 2003; revision received 21 August 2004; accepted for publication 13 September 2004.

*Vice President, 303 Butler Farm Road, Suite 104 A; seywald@ama-inc.com.

†Aerospace Engineer, Mail Stop 328; c.m.roithmayr@larc.nasa.gov.

‡Senior Aerospace Engineer, Mail Stop 328; p.a.troutman@larc.nasa.gov.

§Associate Professor, Center for Astrodynamics and Space Technology, Department of Astronomy and Space Science; spark@galaxy.yonsei.ac.kr. Senior Member AIAA.

¶Data available online at http://spaceflight.nasa.gov/mars/technology/propulsion/aspl/vasimr.html.

orbital transfer is calculated as an explicit function of the prescribed boundary values for the initial and final semimajor axes. The optimization is then performed through variational methods such as those discussed in Refs. 9–13 to determine the optimal thrust history that achieves the prescribed velocity increment with minimum fuel expenditure. The analytical results presented in this paper provide fast and relatively accurate approximations to the trajectory performance.

II. Problem Formulation

The following subsections describe the orbital dynamics and the assumed characteristics of the VASIMR.

A. Equations of Motion

We consider the motion of a spacecraft orbiting in an inverse square gravitational field with the thrust always parallel to the velocity vector. Explicitly, the equations of motion are

$$\dot{\boldsymbol{r}} = \boldsymbol{v} \tag{1}$$

$$\dot{\boldsymbol{v}} = -\mu \cdot \boldsymbol{r}/r^3 + T/m \cdot \boldsymbol{v}/v \tag{2}$$

$$\dot{m} = -|T|/v_e \tag{3}$$

where $\boldsymbol{r}$ and $\boldsymbol{v}$ denote the spacecraft position and velocity vectors, respectively, and the scalars r and v denote the magnitudes of these vectors, that is, $r = \sqrt{(\boldsymbol{r} \cdot \boldsymbol{r})}$, $v = \sqrt{(\boldsymbol{v} \cdot \boldsymbol{v})}$. Furthermore, m denotes the spacecraft mass, the constant μ denotes the central body's gravitational constant, and v_e denotes the exhaust velocity. Note that, in this paper, the thrust magnitude T can take on positive as well as negative values. Positive values of T refer to the case where the thrust is directed along the velocity vector, and negative values of T refer to the case where the thrust is directed opposite to the velocity vector.

Specifically, we are concerned with minimizing the fuel consumption of a VASIMR-powered spacecraft in a circular-to-circular orbit transfer.

B. Description of VASIMR Engine

The VASIMR engine is an electric propulsion system. For constant power input into the engine, it is anticipated that the specific impulse will be throttleable between 3000 and 30,000 s. Clearly, the kinetic energy stored in the expelled mass increases quadratically with the specific impulse I_{sp}, whereas the generated momentum increases linearly with I_{sp}. Explicitly, given a constant input power P, and assuming a constant efficiency factor $q \in [0, 1]$ for the ratio of engine input power P to the kinetic energy deposited in the expelled mass per unit time, we get $q \cdot P = -1/2\dot{m}v_e^2$, where v_e denotes the exhaust velocity at which the fuel mass is expelled, and $\dot{m}$ denotes the mass flow rate. With $\dot{m} = |T|/v_e$ and

$$v_e = I_{sp} \cdot g \tag{4}$$

where T denotes the thrust and g denotes the Earth's gravitational acceleration, this yields after solving for the thrust magnitude $|T|$:

$$|T| = 1/I_{sp} \cdot 2qP/g \tag{5}$$

III. Calculation of the Required Velocity Increment

In this paper, we are concerned with finding the optimal thrust history for achieving a planar circular-to-circular orbital transfer with the VASIMR engine discussed in the preceding section. A complicating feature of the VASIMR engine as well as any other high-I_{sp} engine is that it produces only low levels of thrust with the limited power input typically available in today's spacecraft. More precisely, the thrust magnitude produced by the VASIMR engine is typically small compared to the gravitational forces. This feature poses special challenges for the trajectory optimization as the optimal solution typically involves many orbital revolutions and hence involves many local minima.

In the current section we use the low-thrust assumption to simplify the equations of motion governing the planar circular-to-circular orbital transfer. This leads to an expression for the velocity increment required to perform the transfer that depends only on the initial semimajor axis, the final semimajor axis, and the gravitational constant associated with the central body. In a later section we use this result to formulate an optimal control problem to achieve a prescribed velocity increment with minimum fuel.

A. Evolution of Semimajor Axis

Let r and v denote the spacecraft's radial distance from the central body and the magnitude of the relative inertial velocity with respect to the central body, respectively. The semimajor axis a is defined by

$$a = (2/r - v^2/\mu)^{-1} \tag{6}$$

Differentiating Eq. (6), and using the equations of motion (1) and (2), yields after some simple manipulations

$$\dot{a}(t) = 2\frac{T(t)a(t)^2v(t)}{m(t)\mu} \tag{7}$$

Note that the exhaust velocity v_e does not appear in Eq. (7). Moreover, the thrust magnitude $T(t)$ can be any function of time and/or states.

B. Approximate Evolution of Semimajor Axis Under Low-Thrust Assumptions

We now assume that the spacecraft is initially in a circular orbit about the central body, that the thrust magnitude T is small compared to the gravitational force acting on the spacecraft, and that the thrust is applied throughout the course of each orbit in a manner such that the orbit remains essentially circular.

As a result of these assumptions, the orbit will remain close to circular at all times. Hence the velocity v will always remain close to the velocity associated with a circular orbit, that is, we can approximate $v \approx \sqrt{(\mu/a)}$ Inserting this in Eq. (7), we obtain

$$\dot{a}/2 \cdot \sqrt{\mu}\Big/\sqrt{a(t)^3} = T/m \tag{8}$$

C. Definition of Velocity Increment

The right-hand side of Eq. (8) represents the thrust acceleration that the vehicle would experience in inertial space, without any external forces other than the thrust acting on the vehicle. The integral of the absolute value of this acceleration is commonly referred to as the velocity increment ΔV, that is,

$$\Delta\dot{V} = |T/m|, \qquad \Delta V(t_0) = 0 \tag{9}$$

or

$$\Delta V(t) = \int_{t_0}^{t} \left|\frac{T}{m}\right| \mathrm{d}t \tag{10}$$

D. Velocity Increment Required for Low-Thrust Near-Circular Spiral Transfers

Because, for our application, the thrust T is either always positive or always negative, we can write Eq. (10) in the form

$$\Delta V = \left| \int_{t_0}^{t} -\frac{T}{m}\,\mathrm{d}t \right|$$

Integrating both sides of Eq. (8) from t_0 to t_f yields

$$\sqrt{\frac{\mu}{a_0}} - \sqrt{\frac{\mu}{a_f}} = \int_{t_0}^{t_f} -\frac{T}{m}\,\mathrm{d}t$$

Hence, in terms of the velocity increment ΔV we obtain

$$\left|\sqrt{\mu/a_0} - \sqrt{\mu/a_f}\right| = \Delta V \tag{11}$$

Here we use the short-hand notation $a(t_0) = a_0$ for the initial semimajor axis and $a(t_f) = a_f$ for the final semimajor axis. Equation (11) provides the velocity increment ΔV required to change the semimajor axis of a circular orbit from a_0 to a_f in a low-thrust spiral transfer with the thrust always parallel to the velocity vector. This expression is in agreement with Eq. (3.66) of Ref. 14.

Note that this velocity increment does not represent the correct sign for the change in velocity that the vehicle achieves. For example, for a vehicle in a circular orbit thrusting along the velocity vector leads to an increase in the orbital altitude and hence to a decrease in the velocity, whereas the velocity increment

$$\Delta V = \int \left|\frac{T}{m}\right| \mathrm{d}t$$

as defined in Eq. (10) is always positive.

Interestingly, Eq. (11) shows that the velocity increment required to perform the transfer is completely independent of the exhaust velocity and the thrust. In fact, our derivation of Eq. (11) allows the thrust and the exhaust velocity to be arbitrary functions of states and time, as long as the following low-thrust assumptions remain satisfied:

1) The direction of thrust is either always in the same direction as the velocity vector or always in the opposite direction.

2) The thrust is always small in magnitude (compared to the gravitational force) acting on the vehicle.

3) If the thrust varies with time, it is applied along the orbit such that the intermediate orbit always remains near circular.

IV. Minimization of Fuel Required to Achieve Fixed Velocity Increment

It was shown in the preceding section that the velocity increment

$$\Delta V = \int \left|\frac{T}{m}\right| \mathrm{d}t$$

defined in Eq. (10) required to perform a circular-to-circular low-thrust orbital transfer depends only on the initial semimajor axis and the final semimajor axis but not on the actual thrust level or on the specific impulse function of time. Hence, if we want to minimize the fuel consumption required for a given planar circular-to-circular orbital transfer, it suffices to minimize the fuel consumption required to achieve a given velocity increment.

In the following, we formulate an optimal control problem to determine the optimal thrust history and the associated specific-impulse function of time to achieve a given velocity increment in a given time with minimum fuel expenditure. The thrust magnitude $|T|$ takes on the role of a control variable as it can be selected at will at every instant of time, within bounds determined by Eq. (5) and the bounds on the specific impulse. Following Eqs. (3) and (9), the relevant differential equations for this problem are $\dot{m} = -|T|/(I_{sp}g)$ and $\Delta\dot{V} = |T|/m$, respectively. Note that the thrust magnitude and the specific impulse are related by Eq. (5), so that the first differential equation can be written in the form $\dot{m} = -|T|^2/(2qP)$. The objective is to find the thrust as a function of time such that the velocity increment ΔV is driven from zero to any specified value ΔV_f within a prescribed time t_f with minimal depletion of the vehicle mass m. Because the thrust appears only in absolute values in this problem, we can drop the absolute values in our equations of motion and consider only positive thrust values. This is done in the following formulation to ease notation, but it does not cause any loss of generality.

Note that we are concerned in the following section only with minimizing the fuel consumption required to achieve a given velocity increment ΔV_f. From the preceding results, it is clear that it is irrelevant whether this velocity increment is used to increase or to decrease the semimajor axis.

A. Formulation of Optimal Control Problem

The objective is to minimize fuel mass (i.e., maximize the final vehicle mass) required to achieve a given velocity increment. With the cost function

$$J = -m(t_f) \tag{12}$$

we can formulate the optimal control problem as follows:

$$\text{minimize} \quad J \tag{13}$$

subject to the differential constraints

$$\dot{m} = -T^2/2qP \tag{14}$$

$$\Delta\dot{V} = T/m \tag{15}$$

the boundary conditions

$$m(0) = m_0 \tag{16}$$

$$\Delta V(0) = 0 \tag{17}$$

$$\Delta V(t_f) = \Delta V_f \tag{18}$$

and the control constraint

$$T \in [T_{\min}, T_{\max}] \tag{19}$$

The final time t_f is given. The explicit relation between the thrust magnitude and the specific impulse, as assumed in this paper, is given by Eq. (5).

B. Variational Optimality Conditions

The treatment of the optimal control problem described by Eqs. (12–19) through variational methods discussed in Refs. 9–13 leads to the following Hamiltonian:

$$H = -\lambda_m(T^2/2qP) + \lambda_{\Delta V}(T/m) \tag{20}$$

The costate equations are

$$\dot{\lambda}_m = -\frac{\partial H}{\partial m} = \lambda_{\Delta V}\frac{T}{m^2}$$

$$\dot{\lambda}_{\Delta V} = -\frac{\partial H}{\partial \Delta V} = 0 \tag{21}$$

and the transversality condition is

$$\lambda_m(t_f) = -1 \tag{22}$$

At every instant of time, the optimal value for the thrust magnitude T is obtained from minimizing the Hamiltonian over all admissible control values $T \in [T_{\min}, T_{\max}]$ with $0 < T_{\min} < T_{\max}$. Along arcs where the control constraint (19) is inactive, the optimal thrust magnitude must hence satisfy[15] $\partial H/\partial T = 0$ and $\partial^2 H/\partial T^2 \geq 0$. The first condition yields the unique solution

$$T^* = (\lambda_{\Delta V}/\lambda_m)(qP/m) \tag{23}$$

and the second condition is satisfied if and only if $\lambda_m \leq 0$. Some simple calculations and careful consideration of the possible signs of λ_m and $\lambda_{\Delta V}$ show that the overall control logic is given by

$$T = \begin{cases} T_{\min} & \text{if} \quad T^* < T_{\min}, \\ T^* & \text{if} \quad T^* \in [T_{\min}, T_{\max}], \quad \lambda_m < 0 \\ T_{\max} & \text{if} \quad T^* > T_{\max}, \end{cases} \tag{24}$$

Clearly, Eq. (23) still involves the costates λ_m and $\lambda_{\Delta V}$. To obtain the numerical value of the optimal control setting at any time along the trajectory, it is required to solve the boundary-value problem consisting of the state equations (14) and (15), the costate equations (21), the boundary conditions (16–18), and the transversality condition (22) with the control logic (23) and (24) inserted.

It is well known[16] that for any state x the associated costate λ_x evaluated at time t represents the sensitivity of the final cost J with respect to perturbations in the state x at time t, that is,

$$\lambda_x(t) = \frac{\partial J}{\partial x(t)} \tag{25}$$

From this it is clear that for the present problem (with reasonable boundary conditions) both costates, λ_m and $\lambda_{\Delta V}$, will be negative for all times, that is,

$$\lambda_m(t) < 0 \qquad \forall t, \qquad \lambda_{\Delta V}(t) < 0 \qquad \forall t \tag{26}$$

In the following section we turn our attention to the problem of finding a closed-form analytical solution to the optimal control problem described by Eqs. (12–19). We start with the case where the control constraint (19) never becomes active.

C. Analytical Solution in Unconstrained Case

In the current section we consider the case where the control constraint (19) never becomes active. That means we assume the thrust value T^* given by Eq. (23) always satisfies the constraint $T_{\min} \le T^* \le T_{\max}$ throughout the trajectory. In addition we assume, for the moment, that the sign conditions (26) are satisfied throughout the trajectory. In the final solution we need to verify that these conditions are in fact satisfied as required, for example, by Eq. (24).

Collecting the state equations (14) and (15), costate equations (21), the physical boundary conditions (16–18), and transversality condition (22), and inserting Eq. (23) for the optimal thrust back into the state and costate equations, leads to the following boundary-value problem:

$$\dot{m} = -\left(\lambda_{\Delta V}^2 \big/ \lambda_m^2\right)(qP/2m^2) \tag{27a}$$

$$\Delta\dot{V} = (\lambda_{\Delta V}/\lambda_m)(qP/m^2) \tag{27b}$$

$$\dot{\lambda}_m = \left(\lambda_{\Delta V}^2 \big/ \lambda_m\right)(qP/m^3) \tag{27c}$$

$$\dot{\lambda}_{\Delta v} = 0 \tag{27d}$$

$$m(0) = m_0 \tag{28a}$$

$$\Delta V(0) = 0 \tag{28b}$$

$$\Delta V(t_f) = \Delta V_f \tag{28c}$$

$$\lambda_m(t_f) = -1 \tag{28d}$$

with t_f, ΔV_f, and m_0 given. The boundary-value problem described by Eqs. (27) and (28) can be solved analytically. Namely, solving Eq. (27a) for $\lambda_{\Delta V}^2$ and inserting the result into the Eq. (27c) yields $\dot{\lambda}_m/\lambda_m = -2\dot{m}/m$. Integrating from t to t_f and using the boundary condition (28d) and the property (26), this yields $\lambda_m(t) = -m(t)^{-2} \cdot m(t_f)^2$. Inserting this result back into the differential equations (27) enables also the analytical integration of the remaining quantities. Making use of the boundary conditions in Eqs. (28) yields the unique solution

$$m(t) = \left(\frac{1}{m_0} + \frac{\Delta V_f^2}{2qPt_f^2}t\right)^{-1} \tag{29}$$

$$\Delta V(t) = \frac{\Delta V_f}{t_f} \cdot t \tag{30}$$

$$\lambda_m(t) = -\frac{m(t_f)^2}{m(t)^2} \tag{31}$$

$$\lambda_{\Delta V}(t) = -\frac{\Delta V_f m(t_f)^2}{qPt_f} \tag{32}$$

Inserting the results of Eqs. (29–32) back into Eq. (23), we get the optimal thrust time history in terms of quantities that are explicitly known through the problem formulation, namely,

$$T^*(t) = \left(\frac{1}{m_0} + \frac{\Delta V_f^2}{2qPt_f^2}t\right)^{-1} \cdot \frac{\Delta V_f}{t_f} = m(t)\frac{\Delta V_f}{t_f} \tag{33}$$

and for the associated optimal specific-impulse function of time, we obtain

$$I_{\mathrm{sp}}^*(t) = \frac{2qPt_f}{g\Delta V_f} \cdot \left(\frac{1}{m_0} + \frac{\Delta V_f^2}{2qPt_f^2}t\right) = \frac{2qPt_f}{g\Delta V_f m(t)} \tag{34}$$

Recall that the analytical solution (29–33) derived in this section is based on the optimal thrust history (23) derived for the case that the control constraint (19) is not active. As summarized in Eq. (24), this requires the costate λ_m to be negative for all times. This condition is clearly satisfied in the solution obtained here, as can be seen in Eq. (31). In summary, it has been shown that Eqs. (29–33) furnish the optimal solution to problem (12–19) as long as the thrust program (33) satisfies the bounds (19) for all times $t \in [0, t_f]$. The latter condition obviously represents a requirement on the thrust bounds $T_{\min}$ and $T_{\max}$, respectively.

D. Constrained Case

We now assume that the control constraint (19) becomes active throughout or along some portion of the optimal solution.

Following Eq. (24), the optimal thrust setting is constant along arcs where the control constraint (19) is active, namely, either $T = T_{\min}$ or $T = T_{\max}$. In these cases, the state and costate equations are of the form

$$\dot{m} = -T^2/2qP, \qquad \Delta\dot{V} = T/m$$
$$\dot{\lambda}_m = \lambda_{\Delta V}(T/m^2), \qquad \dot{\lambda}_{\Delta v} = 0 \tag{35}$$

Note that in Eq. (35) the thrust T is constant with either $T = T_{\min}$ or $T = T_{\max}$. Along arcs where the control constraint (19) is inactive, the state and costate equations are of the form shown in Eqs. (27), and the optimal thrust magnitude is given by Eq. (23). The overall trajectory consists of one or more segments of unconstrained arcs (27) and constrained arcs (35). The boundary conditions of the overall trajectory remain as in Eqs. (28). At all switching times t_s between constrained and unconstrained arcs, all states and costates, as well as the optimal thrust function of time remain continuous, that is,

$$m\left(t_s^-\right) = m\left(t_s^+\right), \qquad \Delta V\left(t_s^-\right) = \Delta V\left(t_s^+\right), \qquad \lambda_m\left(t_s^-\right) = \lambda_m\left(t_s^+\right)$$
$$\lambda_{\Delta v}\left(t_s^-\right) = \lambda_{\Delta v}\left(t_s^+\right), \qquad T\left(t_s^-\right) = T\left(t_s^+\right) \tag{36}$$

Even when the constraint is active along a portion of the trajectory, during the unconstrained portion the thrust is monotonically decreasing. This can be seen by differentiating T^* with respect to time. Explicitly, from Eq. (23),

$$\frac{\mathrm{d}}{\mathrm{d}t}T^* = -\frac{\lambda_{\Delta V}^3}{2\lambda_m^3}\frac{q^2P^2}{m^4} < 0$$

Together with the continuity condition (36) this shows that the thrust is monotonically decreasing throughout. Clearly, based on these observations, only four different switching structures are possible, namely,

$$\text{switching structure 1:} \qquad T_{\text{free}}$$

$$\text{switching structure 2:} \qquad T_{\max} \to T_{\text{free}}$$

$$\text{switching structure 3:} \qquad T_{\text{free}} \to T_{\min}$$

$$\text{switching structure 4:} \qquad T_{\max} \to T_{\text{free}} \to T_{\min} \tag{37}$$

Here, T_{free} denotes the optimal thrust setting along unconstrained arcs shown in Eq. (23). With the information derived so far in this section, it is straightforward, however tedious, to solve the boundary-value problem associated with the constrained case analytically. The results are not shown here, as no fundamental new insights can be gained from these expressions. Some interesting insights can be gained, however, from the analytical solution of the unconstrained case, switching structure 1 in Eq. (37), as shown in the next section.

V. Discussion and Numerical Results

Before we discuss and analyze the properties of the analytical approximations just derived, we address briefly one of the key assumptions that makes the underlying analysis possible, namely, the assumption that the thrust direction is always parallel or always antiparallel to the velocity vector. Clearly this is not an assumption forced upon us as a result of hardware limitations, which is the case with the assumption that the thrust magnitude is small. Rather, this assumption is based on the conjecture that firing the thruster parallel/antiparallel to the velocity vector is close to optimal. Clearly, firing the thruster parallel/antiparallel to the velocity provides the largest local increase/decrease in the spacecraft's mechanical energy. However, this argument does not prove optimality of this control strategy for the overall transfer. In fact, in absence of a constraint on the overall time to complete a given circular-to-circular orbital transfer, it is easy to construct low-thrust solutions that have the same low-ΔV requirement as Hohmann transfers. But such low-thrust solutions would require exceedingly long flight times. The solutions presented here are reasonably fast transfers. The authors believe that the solutions presented here are close to fuel optimal. Allowing the thrust direction to vary can yield an optimal trajectory, but as Melbourne notes in Ref. 17, "experience has shown that the improvement in vehicle performance over a straightforward tangential or circumferential constant thrust program is very slight." Herman and Conway[18] obtain an optimal Earth–moon transfer by varying thrust direction; however, their work differs significantly from ours in that a third-body perturbation is included and I_{sp} is regarded as constant.

A. Basic Features of Optimal Transfer in Unconstrained Case

In Eq. (11), we have seen that the velocity increment associated with a low-thrust, circular-to-circular orbital transfer depends only on the initial and final value of the semimajor axis, but is independent of the specific impulse or the thrust magnitude, just as long as the thrust is always directed parallel to the velocity vector and the thrust time history is such that the orbit remains near circular throughout the transfer. The explicit dependence of the velocity increment required to perform such a transfer between the prescribed initial and final values of the semimajor axis is shown in Eq. (11). Based on this result, we then formulated in Sec. IV an optimal control problem to achieve a prescribed velocity increment ΔV_f within a prescribed maneuver time t_f with minimum fuel expenditure. Specifically for the VASIMR engine, where the functional relation between specific impulse and thrust magnitude is given by Eq. (5), we obtained the optimal time histories for the thrust magnitude and the associated specific impulse as shown in Eqs. (33) and (34). Interestingly, the optimal thrust time history and the associated specific-impulse time history are not constant. The optimal solution shows that, as a rule of thumb, higher thrust, at the cost of a lower specific impulse, is used in the beginning of the transfer. Notably, the optimal thrust history is the same for spiraling inward as well as for spiraling outward. Specifically, we make the following observations regarding the optimal solution expressed by Eqs. (29–34):

1) The optimal thrust magnitude T^* is always proportional to the mass m.

2) The resulting thrust acceleration T^*/m is constant, namely, $T^*/m = \Delta V_f/t_f$. Note that this acceleration represents only a hypothetical change in velocity that the spacecraft would experience if it were operating in the absence of other forces. However, as the spacecraft is operating in a circular orbit in an inverse square gravitational field, firing low-thrust thrusters along the velocity vector, for example, would cause the spacecraft to continuously slow down rather than to increase its orbital speed.

3) The specific impulse I_{sp}^* is linear in time.

Recall also that we assumed the control constraint (19) does not become active. In other words, it is assumed that the engine is, in fact, able to generate the thrust levels required by the optimal thrust program (33). It is easy to verify that the optimal thrust is strictly monotonically decreasing with time. Hence, the lowest and highest thrust levels associated with the optimal program appear at the final time and at the initial time of the transfer, respectively. Explicitly, these maximum and minimum thrust values are

$$T(0) = m_0 \Delta V_f / t_f \tag{38}$$

$$T(t_f) = m_f \Delta V_f / t_f \tag{39}$$

Interestingly, the results shown in Sec. IV imply that the fuel consumption for a given orbital transfer is independent of the thrust magnitude. Clearly, by inserting $t = t_f$ into Eq. (29), we find that the final mass fraction obtained for the optimal solution is given by

$$\frac{m_f}{m_0} = \left(1 + \frac{\Delta V_f^2 m_0}{2qPt_f}\right)^{-1} \tag{40}$$

Clearly, the velocity increment is completely independent of the actual thrust magnitude T, just as long as the thrust magnitude is always low enough to qualify as low thrust. The solution represented by Eqs. (29–34) shows in detail how the actual transfer is performed optimally with a low-thrust variable-specific-impulse engine whose specific impulse and thrust magnitude are related through Eq. (5). Obviously, the choice of the thrust magnitude along the optimal transfer is relevant, as an increase in thrust magnitude causes a reduction in the specific impulse and hence a reduction in the fuel efficiency by virtue of Eq. (5). However, as can be seen from Eq. (5), an increase in the power level P enables a proportionate increase in the thrust magnitude T without affecting the specific impulse I_{sp}. In fact, from Eq. (40) it can be seen that changing the power P by any factor $Q > 0$ and altering the maneuver time t_f by a factor $1/Q$ keeps the final mass fraction m_f/m_0 unchanged. Furthermore, from Eq. (33) it is easy to verify that the optimal thrust magnitude changes by a factor of Q uniformly throughout the trajectory.

B. Comparison to Constant-Thrust Transfers

An interesting question to ask is how much fuel is saved through the variable thrust capability alone, compared to a simple fixed-thrust solution. To answer this question, we compare the final mass fraction in Eq. (40) with the final mass fraction achieved for a transfer with the same boundary conditions and with the same prescribed maneuver time but with constant thrust.

To determine the thrust value required for this purpose, we now consider the initial value problem (14–17) for the case of constant thrust T. Using Eq. (15) to eliminate one of the two factors T in Eq. (14), and using Eqs. (4) and (5) to eliminate the second factor, we obtain

$$\dot{m}/m = -\Delta \dot{V}/v_\varepsilon \tag{41}$$

Integrating Eq. (41) with the initial conditions (16) and (17) yields the well-known rocket equation

$$m(t) = m_0 \cdot \exp[-|\Delta V(t)|/v_e] \tag{42}$$

From Eqs. (14) and (16) it is clear that the mass $m(t)$ is also given by

$$m(t) = m_0 - (T^2/2qP) \cdot t \tag{43}$$

Equating the right-hand sides of Eqs. (42) and (43), both evaluated at the final time t_f, yields after some rearranging

$$T = \sqrt{(2qp/t_f) \cdot m_0 \cdot \{1 - \exp[-(|\Delta V_f|/v_e)]\}} \tag{44}$$

We assume that the thrust, specific impulse, and exhaust velocity are constant and, just as in the case of variable thrust, related to one another by Eqs. (4) and (5). Explicitly, Eqs. (4) and (5) imply that

$$v_e = 2qP/T \tag{45}$$

Thus, the thrust magnitude T appears also on the right-hand side of Eq. (44), and Eq. (44) cannot be solved analytically for T. Equation (44) has to be solved iteratively. Once T is obtained, the exhaust velocity v_e can then be obtained from Eq. (45), and the final mass fraction m_f/m_0 can be obtained from Eq. (42), namely,

$$m_f/m_0 = \exp(-|\Delta V_f|/v_e) \tag{46}$$

In the following section, this final mass fraction for the constant-thrust case is compared to that obtained for the optimal variable thrust case.

C. Numerical Example

In the following, we compare the final mass fraction in Eq. (40) obtained for the optimal low-thrust circular-to-circular orbital transfers to the final mass fraction in Eq. (46) obtained for the constant-thrust case. Explicitly, we consider an Earth escape trajectory and an initial mass $m_0 = 37{,}500$ kg, an engine power $P = 35{,}193.463$ W, and an engine efficiency $q = 0.5$. The thrust constraints are assumed inactive so that $T_{\min}$ and $T_{\max}$ are not specified. The final velocity increment ΔV_f is prescribed at values between 1 and 5 km/s, and the maneuver time is prescribed at values ranging from 50 to 100 days. Figure 1 shows the optimal final mass fraction achieved with variable thrust, Eq. (40). The suboptimal final mass fraction (46) [with T and v_e obtained from Eqs. (44) and (45)] achieved with constant thrust is, of course, always less or at best equal. The difference between the optimal and the suboptimal final mass fraction is shown in Fig. 2.

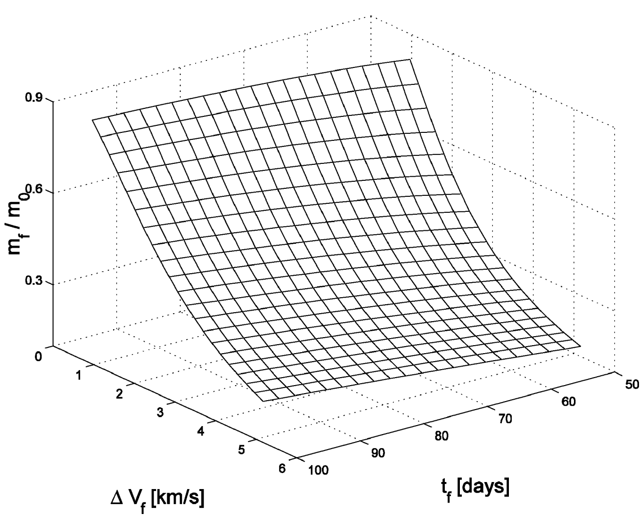

Fig. 1 Optimal final mass fraction achieved with variable thrust. Results are shown for a range of prescribed values for the final velocity increment and the maneuver time.

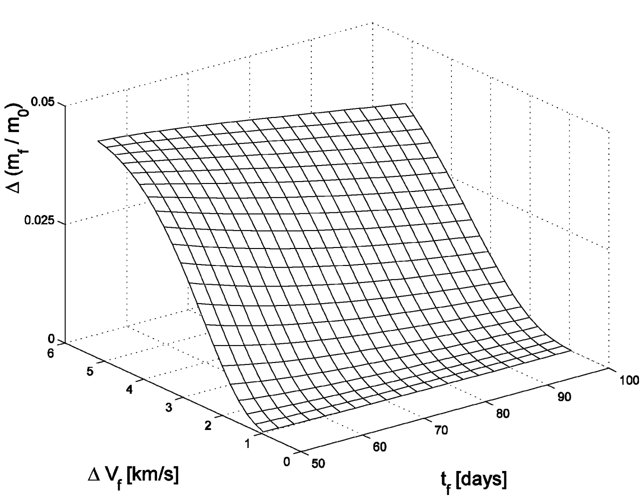

Fig. 2 Improvement in final mass fraction achieved with variable impulse compared to fixed specific impulse. Results are shown for a range of prescribed values for the final velocity increment and the maneuver time.

VI. Conclusions

A fuel optimal control strategy is developed and analyzed for any variable-specific-impulse system, and the strategy is applied to the variable-specific-impulse rocket engine. For planar, time-constrained, circular-to-circular, low-thrust orbital transfers it is shown that the optimal thrust setting is always proportional to the vehicle mass. That means the vehicle thrust acceleration remains constant throughout a transfer, whether the spiral is inward or outward. We also investigate how much fuel is saved with this control logic compared to a constant thrust solution. The explicit percentage of fuel savings depends strongly on the boundary conditions, that is, on the flight time, and the initial and final values of the semimajor axis.

References

[1] Chang Diaz, F. R., Squire, J. P., Ilin, A. V., McCaskill, G. E., Nguyen, T. X., Winter, D. S., Petro, A. J., Goebel, G. W., Cassady, L. D., Stokke, K. A., Dexter, C. E., Graves, T. P., Amador, L., Jr., George, J. A., Carter, M. D., Baity, F. W., Jr., Barber, G. C., Goulding, R. H., Sparks, D. O., Schwenterly, S. W., Bengston, R. D., Breizman, B. N., Jacobson, V. T., Arefiev, A. V., Sagdeev, R. Z., Karavasilis, K., Novakovski, S. V., Chan, A. A., and Glover, T. W., "The Development of the VASIMR Engine," International Conf. on Electromagnetics in Advanced Applications, ICEAA, Turin, Italy, Sept. 1999.

[2] Chang-Diaz, F. R., Squire, J. P., Bengtson, R. D., Breizman, B. N., Baity, F. W., and Carter, M. D., "The Physics and Engineering of the VASIMR Engine," AIAA Paper 2000-3756, July 2000.

[3] Battin, R. H., *An Introduction to the Mathematics and Methods of Astrodynamics*, AIAA, New York, 1987, pp. 396, 416–418.

[4] Stewart, D. J., and Melton, R. G., "Approximate Analytic Representations for Low-Thrust Trajectories," *Advances in the Astronautical Sciences*, Vol. 76, 1991, pp. 1455–1467.

[5] Sukhanov, A. A., and Prado, A. F. B. A., "Constant Tangential Low-Thrust Trajectories near an Oblate Planet," *Journal of Guidance, Control, and Dynamics*, Vol. 24, No. 4, 2001, pp. 723–731.

[6] Kiforenko, B. M., Pasechnik, Z. V., Kyrychenko, S. B., and Vasiliev, I. Y., "Minimum Time Transfer of a Low-Thrust Rocket in Strong Gravity Fields," *Acta Astronautica*, Vol. 52, No. 8, 2003, pp. 601–611.

[7] Xin, W., and Lin, L., "Analytical Solution of Low Thrust Transfer Orbit," International Astronautical Federation, IAC Paper 03-A.P.05, Sept.–Oct. 2003.

[8] Fernandes, S. D. S., "Optimum Low-Thrust Limited Power Transfers between Neighbouring Elliptic Non-Equatorial Orbits in a Non-Central Gravity Field," *Acta Astronautica*, Vol. 35, No. 12, 1995, pp. 763–770.

[9] Pontryagin, L. S., Boltyanskii, V. G., Gamkrelidze, R. V., and Mischenko, E. F., *The Mathematical Theory of Optimal Processes*, Wiley-Interscience, New York, 1962.

[10] Bryson, A. E., and Ho, Y. C., *Applied Optimal Control*, Hemisphere, New York, 1975, Chap. 2, 3.

[11] Lee, E. B., and Markus, L., *Foundations of Optimal Control Theory*, Krieger, Malabar, FL, 1986, Chap. 4.

[12] Leitmann, G., *The Calculus of Variations and Optimal Control*, Plenum, New York, 1981, Chap. 9.

[13] Neustadt, L. W., *A Theory of Necessary Conditions*, Princeton Univ. Press, Princeton, NJ, 1976, Chap. 5, pp. 212–242.

[14] Wiesel, W. E., *Spaceflight Dynamics*, 2nd ed., McGraw–Hill, New York, 1997, pp. 90–92.

[15] Gill, P. E., Murray, W., and Wright, M. H., *Practical Optimization*, Academic Press, London, 1981, Sec. 3.2.2, pp. 63–65.

[16] Seywald, H., and Kumar, R. R., "A Finite Difference Scheme for Automatic Costate Calculation," *Journal of Guidance, Control, and Dynamics*, Vol. 19, No. 1, 1996, pp. 231–239.

[17] Melbourne, W. G., "Interplanetary Trajectories and Payload Capabilities of Advanced Propulsion Vehicles," NASA TR 32-68, Jet Propulsion Lab., California Inst. of Technology, Pasadena, 1961, pp. 15, 16.

[18] Herman, A. L., and Conway, B. A., "Optimal, Low-Thrust, Earth-Moon Orbit Transfer," *Journal of Guidance, Control, and Dynamics*, Vol. 21, No. 1, 1998, pp. 141–147.